ELSEVIER

Physica D 166 (2002) 131–146

PHYSICA D

www.elsevier.com/locate/physd

# Bifurcation analysis of a class of first-order nonlinear delay-differential equations with reflectional symmetry

Brian F. Redmond [a], Victor G. LeBlanc [a,*], André Longtin [b]

[a] *Department of Mathematics and Statistics, University of Ottawa, Ottawa, Ont., Canada K1N 6N5*
[b] *Department of Physics, University of Ottawa, Ottawa, Ont., Canada K1N 6N5*

Received 1 August 2001; received in revised form 10 February 2002; accepted 27 February 2002
Communicated by J.P. Keener

**Abstract**

We consider a general class of first-order nonlinear delay-differential equations (DDEs) with reflectional symmetry, and study completely the bifurcations of the trivial equilibrium under some generic conditions on the Taylor coefficients of the DDE. Our analysis reveals a Hopf bifurcation curve terminating on a pitchfork bifurcation line at a codimension two Takens–Bogdanov point in parameter space. We compute the normal form coefficients of the reduced vector field on the centre manifold in terms of the Taylor coefficients of the original DDE, and in contrast to many previous bifurcation analyses of DDEs, we also compute the unfolding parameters in terms of these coefficients. For application purposes, this is important since one can now identify the possible asymptotic dynamics of the DDE near the bifurcation points by computing quantities which depend explicitly on the Taylor coefficients of the original DDE. We illustrate these results using simple model systems relevant to the areas of neural networks and atmospheric physics, and show that the results agree with numerical simulations.


*PACS:* 02.30.Ks; 02.30.Oz; 87.18.Sn; 05.45.−a

*Keywords:* Delay-differential equations; Neural networks; Takens–Bogdanov bifurcation; Centre manifold; Bistable systems; Delayed feedback; ENSO

## 1. Introduction

In this paper, we consider the following DDE

$$\frac{\mathrm{d}}{\mathrm{d}t}x(t) = f(x(t), x(t-\delta)), \tag{1.1}$$

where $\delta > 0$ is the delay, and $f$ is an arbitrary smooth function which has reflectional symmetry in the following sense: $f(-a,-b) = -f(a,b)$ for all real $a$ and $b$. The reflectional symmetry of $f$ in (1.1) implies that $f(0,0) = 0$, i.e. the origin is an equilibrium solution. In this paper, we will be interested in the bifurcations of this trivial

* Corresponding author. Tel.: +613-562-5800x3519; fax: +613-562-5776.
*E-mail address:* vleblanc@mathstat.uottawa.ca (V.G. LeBlanc).
URL: http://aixl.uottawa.ca/∼vleblanc.

0167-2789/02/$ – see front matter 
PII: S0167-2789(02)00423-2

equilibrium. Specifically, we focus on the Taylor expansion of Eq. (1.1) around $(0, 0)$, which yields, after a rescaling of time

$$\frac{\mathrm{d}}{\mathrm{d}t}x(t)=x(t)+\alpha x(t-\tau)+\gamma_1 x(t)^3+\gamma_2 x(t)^2 x(t-\tau)+\gamma_3 x(t)x(t-\tau)^2+\gamma_4 x(t-\tau)^3+\mathrm{O}(|x|^5), \quad (1.2)$$

where $\tau = \mathrm{D}_1 f(0,0)\delta, \alpha = \mathrm{D}_2 f(0,0)/\mathrm{D}_1 f(0,0), \gamma_1 = \mathrm{D}_{111} f(0,0)/6\mathrm{D}_1 f(0,0), \gamma_2 = \mathrm{D}_{112} f(0,0)/2\mathrm{D}_1 f(0,0)$, $\gamma_3 = \mathrm{D}_{122} f(0,0)/2\mathrm{D}_1 f(0,0)$, and $\gamma_4 = \mathrm{D}_{222} f(0,0)/6\mathrm{D}_1 f(0,0)$. In our notation, $\mathrm{D}_i f(0,0)$ denotes the first-order partial derivative of the function $f$ with respect to its $i$th argument ($i = 1, 2$), evaluated at $(0, 0)$, with similar notation used for higher order partial derivatives. Here we have assumed that the Taylor coefficient $\mathrm{D}_1 f(0,0)$ is positive in order to achieve a coefficient of 1 for the $x(t)$ term in (1.2). We will see that in this case codimension one bifurcation curves can intersect, leading to a codimension two bifurcation point. The case where $\mathrm{D}_1 f(0,0) < 0$ can be studied without any added difficulty. However, it is a somewhat simpler case in the sense that the codimension one bifurcation curves do not intersect [3]; it has in fact been previously treated (see e.g. [2,14]).

Eq. (1.2) encompasses a wide variety of possible physical situations. For example, the case

$$\frac{\mathrm{d}x}{\mathrm{d}t} = x - x^3 + \alpha x(t-\tau) \quad (1.3)$$

corresponds to the equation of motion of a particle in an overdamped bistable symmetric potential known as the "standard quartic" potential, with an additional linear force due to its motion in the past. The motion in the absence of delayed feedback has two coexisting fixed points, separated by the unstable origin. Whether this delayed force is restoring or not (with respect to the origin) may depend on its magnitude and sign, which in turn will depend on the full dynamics of the system. In particular, we will see that our bifurcation analysis of such a system reveals parameter regions where the origin is stabilized by this delayed force.

The fact that the origin is unstable even without delayed feedback is a distinguishing feature of the DDE class equation (1.2). This is in contrast with work on e.g. neural circuits and networks with one [2,5,22] or more [6,8,9,15,26–28] delays. Our particular interest in this class of DDEs stems from their relevance to coupled bistable detector arrays [13,20]. Such arrays can use noise and coupling to synchronize transitions between states to the fluctuations of small input signals, thereby amplifying these signals. We are currently extending the coupling of such elements to include delayed feedback. This connectivity is suggested in particular by neural circuitry involved in signal detection and processing (see e.g. [4] and references therein). In this context, it is known that bistable systems are also a good approximation to the dynamics of certain neurons [7,21]. In particular, they have recently been shown to be powerful building blocks for neural networks performing associative memory tasks [10]. Further, there has also been a recent study of combined bistability and delay and noise in the context of a simple neuron model [23].

Thus, inspired by research on bistable systems and on neural dynamics and information processing, we have been developing versions of such neural networks and detector arrays that include delayed feedback. It has become crucial, in this context, to understand the basic dynamics of bistability with feedback. We also anticipate that the dynamics studied here will be of relevance to studies of chemical reactions with global delayed feedback (see [19] and references therein).

Specific instances of Eq. (1.2) have also found applications in atmospheric physics, namely as early heuristic models of the El Niño/southern oscillation (ENSO) phenomenon [1,24]; this "delayed oscillator" approach to ENSO is summarized in Section 5 as a preamble to the examples chosen to illustrate our analytical results. Such models had only been analyzed using linear stability analysis as well as numerical analysis; their full bifurcation analysis had not been done, and in particular, the presence of a codimension two bifurcation point had escaped earlier numerical analyses. Although current models of ENSO are more sophisticated, our analysis of these earlier models

improves our understanding of the dynamical complexity that the delayed oscillator picture may hold in this and other contexts.

The paper is organized as follows. In the next section, we will study the linearized stability of the trivial equilibrium of (1.2), and show that in the $(\alpha, \tau)$-parameter space, there are two codimension one bifurcation curves: a Hopf bifurcation curve and a pitchfork curve. The Hopf curve terminates at the pitchfork curve in a point where the characteristic equation has a double zero root. This corresponds to a codimension two Takens–Bogdanov bifurcation of the trivial equilibrium. In Section 3, we briefly review the theory of centre manifold reduction for parameter dependent DDEs, and then perform centre manifold reductions for both the Hopf and the pitchfork bifurcations in (1.2). In particular, we compute both the first Liapunov coefficient of the Hopf bifurcation, and the coefficient of the cubic term in the pitchfork normal form in terms of the coefficients $\alpha$, $\tau$ and $\gamma_i$, $1 \leq i \leq 4$, of (1.2). In Section 4, we study the Takens–Bogdanov bifurcation for (1.2). Because of the reflectional symmetry of $f$ in (1.1), the centre manifold equations will also have reflectional symmetry. It is well-known that generically, there are two distinct topological types (normal forms) for this bifurcation. As a by-product of our analysis, we will give conditions on the coefficients $\gamma_i$, $1 \leq i \leq 4$, of (1.2) which determine which type of Takens–Bogdanov bifurcation will occur in (1.1). Thus, provided these generic conditions are satisfied, our analysis completely describes the local bifurcations of the trivial equilibrium solution in (1.1), *regardless of the fifth and higher order terms in* (1.2). Finally, in Section 5 we will illustrate our results with some numerical integrations of certain models which fall into the class of equations described by (1.1). A conclusion follows in Section 6.

## 2. Linear stability analysis

In this section, we locate the region of stability of the equilibrium solution $x(t) = 0$ of Eq. (1.2). Linearizing (1.2) near this equilibrium solution we obtain

$$\frac{\mathrm{d}}{\mathrm{d}t}x(t) = x(t) + \alpha x(t-\tau). \tag{2.1}$$

Substitution of the ansatz $x(t) = \mathrm{e}^{\lambda t}$ into (2.1), where $\lambda$ is a complex parameter, gives the characteristic equation

$$\lambda = 1 + \alpha\,\mathrm{e}^{-\lambda\tau}. \tag{2.2}$$

Using Theorem A.5 of [18] we find that all roots of (2.2) have negative real parts if and only if

$$\tau < 1, \qquad \alpha < -1, \qquad \alpha\tau > -\zeta\sin\zeta - \tau\cos\zeta, \tag{2.3}$$

where $\zeta$ is the root of $\zeta = \tau\tan\zeta$, $0 < \zeta < \pi$, and $\zeta = \pi/2$ if $\tau = 0$. Since $\tau$ must be positive (for the physically interesting case), the region defined by (2.3) is illustrated as the hatched region in Fig. 1. On the top and right-hand boundaries of the hatched region in Fig. 1, Eq. (2.2) has a finite number of solutions with zero real part, and all other solutions have negative real part. Therefore, bifurcations occur for parameter values on these two curves. The top boundary curve is characterized by setting $\lambda = \mathrm{i}\omega$ in (2.2). After separating real and imaginary parts in (2.2), we obtain

$$1 = -\alpha\cos\omega\tau, \qquad \omega = -\alpha\sin\omega\tau. \tag{2.4}$$

Squaring both equations and adding, we get

$$\omega = \pm\sqrt{\alpha^2 - 1}. \tag{2.5}$$

The right-hand boundary curve is characterized by setting $\lambda = 0$ in (2.2). This substitution gives

$$\alpha = -1. \tag{2.6}$$

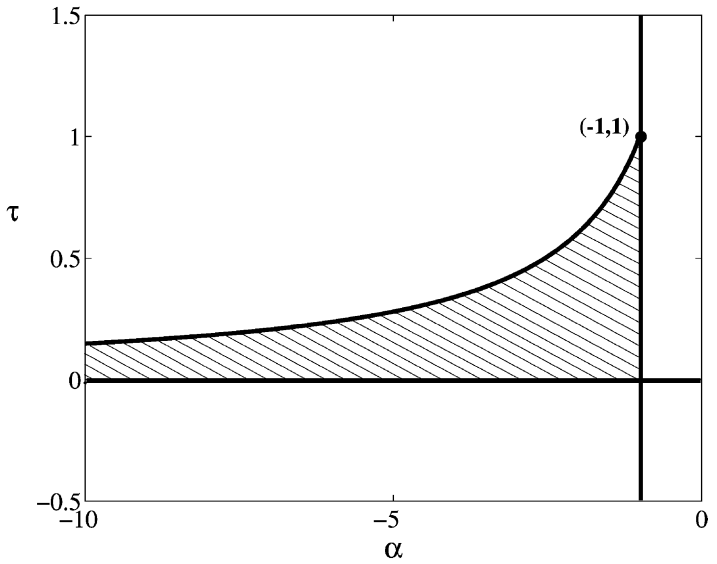


Fig. 1. Stability diagram for the equilibrium solution $x(t) = 0$ of (1.2). Hatched area corresponds to the stability region.

We see that the right boundary line $\alpha = -1$ in Fig. 1 is a line where the characteristic equation has a single zero root. Because of the reflectional symmetry of (1.2), this line corresponds to a pitchfork bifurcation curve. The top boundary curve in Fig. 1 is a curve where the characteristic equation has purely imaginary complex conjugate roots (i.e. it is a Hopf bifurcation curve). At the point $(\alpha, \tau) = (-1, 1)$ where these two curves meet, (2.2) has a double zero root, i.e. (2.1) has two linearly independent solutions $x(t) = 1$ and $x(t) = t$. This point thus corresponds to a Takens–Bogdanov bifurcation.

## 3. Centre manifold reduction for DDEs

In this section, we briefly summarize the theory for centre manifold reductions of DDEs with parameters (see e.g. [11,12,17,18]), and then apply these results to compute normal forms for both the Hopf and pitchfork bifurcations of the trivial equilibrium in (1.2). We will perform a similar analysis for the Takens–Bogdanov bifurcation in the next section.

We first let $X \stackrel{\text{def}}{=} C([-\tau, 0], \mathbb{R}^{1+p})$, $\tau \geq 0$ denote the space of continuous functions from the interval $[-\tau, 0]$ into $\mathbb{R}^{1+p}$. Consider the following autonomous DDE

$$\frac{\mathrm{d}}{\mathrm{d}t} y(t) = \mathcal{L} y_t + F(y_t), \quad t \geq 0, \tag{3.1}$$

where $y_t(\theta) = [x(t+\theta), \mu_1(t+\theta), \ldots, \mu_p(t+\theta)]^{\mathrm{T}} \in X$, $-\tau \leq \theta \leq 0$, $\mathcal{L} : X \to \mathbb{R}^{1+p}$ is a bounded linear operator, and $F \in C^r(X, \mathbb{R}^{1+p})$, $r \geq 1$ is some smooth nonlinearity with $F(0) = 0$ and $\mathrm{D}F(0) = 0$. Note that (3.1) should be viewed as a suspended system where the $p$ parameters are included as dynamic variables with trivial dynamics. For our purposes, the dimension $p$ of the parameter space for the suspended system will equal 1 or 2, depending on the bifurcation under study. The linearization of Eq. (3.1) about the trivial equilibrium is given by

$$\frac{\mathrm{d}}{\mathrm{d}t} y(t) = \mathcal{L} y_t, \quad t \geq 0. \tag{3.2}$$

Since $\mathcal{L}$ is a bounded linear operator from $X$ to $\mathbb{R}^{1+p}$, it follows from Riesz's theorem that $\mathcal{L}$ can be represented by a Riemann–Stieltjes integral

$$\mathcal{L}\phi = \int_{-\tau}^{0} [\mathrm{d}\eta(\theta)]\phi(\theta), \quad \phi \in X, \tag{3.3}$$

where $\eta(\theta)$, $-\tau \leq \theta \leq 0$, is a $(1+p) \times (1+p)$ matrix whose elements are of bounded variation.

We may then rewrite Eq. (3.2) in the following form

$$\frac{\mathrm{d}}{\mathrm{d}t} y(t) = \int_{-\tau}^{0} [\mathrm{d}\eta(\theta)] y(t+\theta), \quad t \geq 0. \tag{3.4}$$

Define $X' = C([0, \tau], \mathbb{R}^{(1+p)*})$, where $\mathbb{R}^{(1+p)*}$ is a space of row vectors. The transpose of Eq. (3.4) is

$$\frac{\mathrm{d}}{\mathrm{d}t} y(t) = -\int_{-\tau}^{0} y(t-\theta)[\mathrm{d}\eta(\theta)], \quad t \geq 0, \qquad y_0 = \psi \in X'. \tag{3.5}$$

For $\phi \in X$ and $\psi \in X'$, the following bilinear form is defined

$$\langle \psi, \phi \rangle = \psi(0)\phi(0) - \int_{-\tau}^{0} \int_{0}^{\theta} \psi(\xi - \theta)[\mathrm{d}\eta(\theta)]\phi(\xi)\,\mathrm{d}\xi. \tag{3.6}$$

In the definition of the bilinear form as stated above, the integral over $\mathrm{d}\eta(\theta)$ is performed last (with integration limits $-\tau$ to 0).

Since (3.1) has $p$ components with trivial dynamics, then the characteristic equation corresponding to Eq. (3.2) always has $p$ eigenvalues on the imaginary axis (at the origin). Thus, at a bifurcation, this characteristic equation has $m+p$ eigenvalues (counting multiplicity) on the imaginary axis and we will assume that all other eigenvalues have negative real parts. Then there exists an $(m+p)$-dimensional centre subspace $P \subset X$ for Eq. (3.4) which is invariant under the semi-flow for (3.2). We will denote a basis for $P$ by the $(1+p) \times (m+p)$ matrix $\Phi$; the columns of $\Phi$ are the basis vectors. There is a corresponding $(m+p)$-dimensional subspace $P'$ of $X'$ of solutions to the transposed equation (3.5). We will denote a basis for $P'$ by the $(m+p) \times (1+p)$ matrix $\Psi'$. Hale and Lunel [18] have shown that the $(m+p) \times (m+p)$ matrix $\langle \Psi', \Phi \rangle$ is always non-singular. We then define a new basis $\Psi$ for $P'$ by $\Psi = \langle \Psi', \Phi \rangle^{-1} \Psi'$ so that $\langle \Psi, \Phi \rangle = I$. The space $X$ can be split as

$$X = P \oplus Q,$$

where $Q$ is infinite-dimensional and invariant under the semi-flow for (3.2). It can then be shown using integral manifold techniques [18] that there exists an $(m+p)$-dimensional centre manifold $M_F$ for Eq. (3.1) given by

$$M_F = \{\phi \in X : \phi = \Phi z + h(z, F), \quad z \text{ in a neighbourhood of zero in } \mathbb{R}^{m+p}\},$$

where $h(z, F) \in Q$ for each $z$ and is a $C^{r-1}$ function of $z$. The flow on this centre manifold is given by

$$y_t = \Phi z(t) + h(z(t), F),$$

and $z$ satisfies the ordinary differential equation

$$\frac{\mathrm{d}}{\mathrm{d}t} z = Bz + \Psi(0) F(\Phi z + h(z, F)), \tag{3.7}$$

where the $(m+p) \times (m+p)$ matrix $B$ satisfies the relation

$$\frac{\mathrm{d}}{\mathrm{d}\theta} \Phi = \Phi B. \tag{3.8}$$

The flow of Eq. (3.7) approximates well the long term behaviour of the flow of the full nonlinear system (3.1) near the origin. This is the framework in which we will study the bifurcations of the trivial equilibrium in (1.1).

### 3.1. Pitchfork bifurcation

We have seen in the previous section that the trivial equilibrium for (1.2) undergoes a pitchfork bifurcation when $\alpha = -1$ and $\tau \neq 1$. Thus, in this section, we treat $\alpha$ as a bifurcation parameter near $-1$, and we assume that $\tau$ is fixed and not equal to 1. We thus have $m = 1$ and $p = 1$. Using the formalism of the previous subsection, we may rewrite Eq. (1.2) in the following form

$$\begin{aligned}\frac{\mathrm{d}}{\mathrm{d}t}x(t) = {} & x(t) - x(t-\tau) + \mu x(t-\tau) + \gamma_1 x(t)^3 + \gamma_2 x(t)^2 x(t-\tau) + \gamma_3 x(t) x(t-\tau)^2 \\ & + \gamma_4 x(t-\tau)^3 + \mathrm{O}(|x|^5), \qquad \frac{\mathrm{d}}{\mathrm{d}t}\mu(t) = 0, \end{aligned} \tag{3.9}$$

where we have set $\alpha = \mu - 1$. Linearizing (3.9) at the trivial equilibrium, we get the following

$$\frac{\mathrm{d}}{\mathrm{d}t}x(t) = x(t) - x(t-\tau), \qquad \frac{\mathrm{d}}{\mathrm{d}t}\mu(t) = 0. \tag{3.10}$$

A basis for the centre subspace of the linear system (3.10) is

$$\Phi = \begin{pmatrix} 1 & 0 \\ 0 & 1 \end{pmatrix},$$

the bilinear form (3.6) for this problem is given by

$$\langle \psi, \phi \rangle = \psi(0)\phi(0) - \int_{-\tau}^{0} \psi(\xi + \tau) \begin{pmatrix} 1 & 0 \\ 0 & 0 \end{pmatrix} \phi(\xi)\, \mathrm{d}\xi, \tag{3.11}$$

and the matrix

$$B = \begin{pmatrix} 0 & 0 \\ 0 & 0 \end{pmatrix},$$

satisfies relation (3.8). Write $z = [z_1, \mu]^{\mathrm{T}}$ for the coordinates on the centre manifold. Finally, we note that the nonlinear terms in (3.9) can be written as

$$\begin{aligned} F([v_1, v_2]^{\mathrm{T}}) = {} & [v_2(0)v_1(-\tau) + \gamma_1 v_1(0)^3 + \gamma_2 v_1(0)^2 v_1(-\tau) + \gamma_3 v_1(0) v_1(-\tau)^2 \\ & + \gamma_4 v_1(-\tau)^3 + \mathrm{O}(|v|^5), 0]^{\mathrm{T}}. \end{aligned} \tag{3.12}$$

Retaining up to first-order terms in $\mu$, and up to third-order terms overall, we get the following equations on the centre manifold

$$\frac{\mathrm{d}}{\mathrm{d}t}z_1 = \frac{1}{1-\tau}[\mu z_1 + (\gamma_1 + \gamma_2 + \gamma_3 + \gamma_4) z_1^3], \tag{3.13}$$

$$\frac{\mathrm{d}}{\mathrm{d}t}\mu = 0. \tag{3.14}$$

Note that $1 - \tau$ is non-zero if and only if $\tau \neq 1$. Thus, the above reduction breaks down (as expected) at this point which, as we will see, is in fact a Takens–Bogdanov point. Generically, the cubic coefficient $(\gamma_1 + \gamma_2 + \gamma_3 + \gamma_4)$

is non-zero, and thus (3.13) is a normal form for a pitchfork bifurcation. In terms of the original model parameters, Eq. (3.13) becomes

$$\frac{\mathrm{d}}{\mathrm{d}t}z_1 = \frac{1}{1-\tau}[(\alpha+1)z_1 + (\gamma_1+\gamma_2+\gamma_3+\gamma_4)z_1^3]. \tag{3.15}$$

### 3.2. Hopf bifurcation

We now suppose that $(\alpha_0, \tau_0)$ is a point on the top boundary curve in Fig. 1. In this case Eq. (2.2) has a pair of purely imaginary roots, and all other roots have negative real parts. We rewrite Eq. (1.2) as

$$\begin{aligned}\frac{\mathrm{d}}{\mathrm{d}t}x(t) &= x(t) + \alpha_0 x(t-\tau_0) + \mu x(t-\tau_0) + \gamma_1 x(t)^3 + \gamma_2 x(t)^2 x(t-\tau_0) + \gamma_3 x(t)x(t-\tau_0)^2 \\ &\quad +\gamma_4 x(t-\tau_0)^3 + \mathrm{O}(|x|^5), \qquad \frac{\mathrm{d}}{\mathrm{d}t}\mu(t) = 0,\end{aligned} \tag{3.16}$$

where we have set $\alpha = \mu + \alpha_0$. The linearization of this equation at the trivial equilibrium is

$$\frac{\mathrm{d}}{\mathrm{d}t}x(t) = x(t) + \alpha_0 x(t-\tau_0), \qquad \frac{\mathrm{d}}{\mathrm{d}t}\mu(t) = 0. \tag{3.17}$$

A basis for the centre subspace of the linear system (3.17) is

$$\Phi = \begin{pmatrix} \sin(\omega_0\theta) & \cos(\omega_0\theta) & 0 \\ 0 & 0 & 1 \end{pmatrix},$$

where $\omega_0 = \sqrt{\alpha_0^2 - 1}$ by (2.5). The bilinear form (3.6) reduces to

$$\langle \psi, \phi \rangle = \psi(0)\phi(0) + \alpha_0 \int_{-\tau_0}^{0} \psi(\xi+\tau_0) \begin{pmatrix} 1 & 0 \\ 0 & 0 \end{pmatrix} \phi(\xi)\,\mathrm{d}\xi, \tag{3.18}$$

and we let

$$\Psi = \langle \Phi^{\mathrm{T}}, \Phi \rangle^{-1}\Phi^{\mathrm{T}} = \kappa \begin{pmatrix} \frac{1}{2}[(1-\tau_0)\sin(\omega_0\theta) + \omega_0\tau_0\cos(\omega_0\theta)] & 0 \\ \frac{1}{2}[-\omega_0\tau_0\sin(\omega_0\theta) + (1-\tau_0)\cos(\omega_0\theta)] & 0 \\ 0 & \kappa^{-1} \end{pmatrix} \stackrel{\mathrm{def}}{=} \begin{pmatrix} b_1(\theta) & 0 \\ b_2(\theta) & 0 \\ 0 & 1 \end{pmatrix}$$

be a basis for the transposed system to Eqs. (3.17), where $\kappa = 4/((1-\tau_0)^2 + (\omega_0\tau_0)^2)$. It can easily be checked that the matrix

$$B = \begin{pmatrix} 0 & -\omega_0 & 0 \\ \omega_0 & 0 & 0 \\ 0 & 0 & 0 \end{pmatrix},$$

satisfies relation (3.8). Write $z = [z_1, z_2, \mu]^{\mathrm{T}}$ for the coordinates on the centre manifold. The nonlinear terms in (3.16) are given by

$$\begin{aligned}F([v_1, v_2]^{\mathrm{T}}) &= [v_2(0)v_1(-\tau_0) + \gamma_1 v_1(0)^3 + \gamma_2 v_1(0)^2 v_1(-\tau_0) + \gamma_3 v_1(0)v_1(-\tau_0)^2 + \gamma_4 v_1(-\tau_0)^3 \\ &\quad +\mathrm{O}(|v|^5), 0]^{\mathrm{T}}.\end{aligned} \tag{3.19}$$

Substituting the above results into Eq. (3.7) and truncating, we get the following ordinary differential equations on the centre manifold

$$\frac{\mathrm{d}}{\mathrm{d}t}z_1 = -\omega_0 z_2 + b_1(0)[\mu(-\sin(\omega_0\tau_0)z_1 + \cos(\omega_0\tau_0)z_2) + \gamma_1 z_2^3 + \gamma_2 z_2^2(-\sin(\omega_0\tau_0)z_1 + \cos(\omega_0\tau_0)z_2) + \gamma_3 z_2(-\sin(\omega_0\tau_0)z_1 + \cos(\omega_0\tau_0)z_2)^2 + \gamma_4(-\sin(\omega_0\tau_0)z_1 + \cos(\omega_0\tau_0)z_2)^3], \tag{3.20}$$

$$\frac{\mathrm{d}}{\mathrm{d}t}z_2 = \omega_0 z_1 + b_2(0)[\mu(-\sin(\omega_0\tau_0)z_1 + \cos(\omega_0\tau_0)z_2) + \gamma_1 z_2^3 + \gamma_2 z_2^2(-\sin(\omega_0\tau_0)z_1 + \cos(\omega_0\tau_0)z_2) + \gamma_3 z_2(-\sin(\omega_0\tau_0)z_1 + \cos(\omega_0\tau_0)z_2)^2 + \gamma_4(-\sin(\omega_0\tau_0)z_1 + \cos(\omega_0\tau_0)z_2)^3], \tag{3.21}$$

$$\frac{\mathrm{d}}{\mathrm{d}t}\mu = 0. \tag{3.22}$$

Now consider the linear part (in $(z_1, z_2)$) of Eqs. (3.20) and (3.21),

$$\frac{\mathrm{d}}{\mathrm{d}t}z = B'z, \tag{3.23}$$

where

$$B' = \begin{pmatrix} -b_1(0)\mu\sin(\omega_0\tau_0) & -\omega_0 + b_1(0)\mu\cos(\omega_0\tau_0) \\ \omega_0 - b_2(0)\mu\sin(\omega_0\tau_0) & b_2(0)\mu\cos(\omega_0\tau_0) \end{pmatrix},$$

and where we have redefined $z$ such that $z = [z_1, z_2]^{\mathrm{T}}$. By a linear change of variables in $z$, the matrix $B'$ can be brought into the following Jordan normal form

$$B'' = \begin{pmatrix} c_1 & -c_2 \\ c_2 & c_1 \end{pmatrix},$$

where, e.g., to first-order in $\mu$

$$c_1 = \tfrac{1}{2}\mu(b_2(0)\cos(\omega_0\tau_0) - b_1(0)\sin(\omega_0\tau_0)). \tag{3.24}$$

After a further (nonlinear) change of variables the equations on the centre manifold can be brought into normal form and truncated at third-order to give

$$\frac{\mathrm{d}}{\mathrm{d}t}z_1 = (c_1 + a(z_1^2 + z_2^2))z_1 - (c_2 + b(z_1^2 + z_2^2))z_2, \tag{3.25}$$

$$\frac{\mathrm{d}}{\mathrm{d}t}z_2 = (c_2 + b(z_1^2 + z_2^2))z_1 + (c_1 + a(z_1^2 + z_2^2))z_2, \tag{3.26}$$

where $a$ and $b$ are constants. In polar coordinates these equations simplify further and become

$$\frac{\mathrm{d}}{\mathrm{d}t}r = c_1 r + a r^3, \tag{3.27}$$

$$\frac{\mathrm{d}}{\mathrm{d}t}\theta = c_2 + b r^2. \tag{3.28}$$

The first Liapunov coefficient $a$ can be computed and is given by

$$a(\mu) = \frac{1}{2[(1-\tau_0)^2 + (\omega_0\tau_0)^2]}\left[\gamma_1\left(\frac{3}{2} - \frac{3\tau_0}{2}\right) + \gamma_2\left(\frac{\alpha_0\tau_0}{2} + \frac{\tau_0}{\alpha_0} - \frac{3}{2\alpha_0}\right) + \gamma_3\left(\frac{1}{2} - \frac{3\tau_0}{2} + \frac{1}{\alpha_0^2}\right) + \gamma_4\left(\frac{3\alpha_0\tau_0}{2} - \frac{3}{2\alpha_0}\right)\right] + \mathrm{O}(\mu), \tag{3.29}$$

where the constants $\alpha_0$, $\tau_0$, and $\omega_0$ are such that Eqs. (2.4) are satisfied.

Eqs. (3.25) and (3.26) are a normal form for the standard Hopf bifurcation provided that the first Liapunov coefficient $a(0)$ and the eigenvalue crossing speed $\partial c_1/\partial\mu|_{\mu=0}$ are both finite and non-zero. We immediately see that this breaks down (as expected) at the point $(\alpha_0, \tau_0) = (-1, 1)$, which will be shown below to be a Takens–Bogdanov point. A straightforward computation reveals that for all $(\alpha_0, \tau_0) \neq (-1, 1)$ on the Hopf curve, we have $\partial c_1/\partial\mu|_{\mu=0} > 0$, so the crossing condition is always satisfied. However, the coefficient $a(0)$ can be zero at isolated points on the Hopf curve away from the Takens–Bogdanov point. The exact places where this occurs will depend on the values of the coefficients $\gamma_i$, $1 \leq i \leq 4$. At such points, (3.25) and (3.26) are no longer a normal form for the Hopf bifurcation (fifth-order terms are required).

## 4. Takens–Bogdanov bifurcation

In this section, we will compute a centre manifold/normal form reduction of (1.2) near the point $(\alpha, \tau) = (-1, 1)$, and show that the trivial equilibrium undergoes a Takens–Bogdanov bifurcation at this point. Since this singularity has codimension 2, we perform the centre manifold suspension with both parameters. By rescaling time in units of the delay we may rewrite Eq. (1.2) in the following form

$$\begin{aligned}\frac{\mathrm{d}}{\mathrm{d}t}x(t) &= x(t) - x(t-1) + \mu_2[x(t) - x(t-1)] + (1+\mu_2)[\mu_1 x(t-1) + \gamma_1 x(t)^3 + \gamma_2 x(t)^2 x(t-1) \\ &\quad + \gamma_3 x(t)x(t-1)^2 + \gamma_4 x(t-1)^3 + \mathrm{O}(|x|^5)], \qquad \frac{\mathrm{d}}{\mathrm{d}t}\mu_1(t) = 0, \qquad \frac{\mathrm{d}}{\mathrm{d}t}\mu_2(t) = 0, \end{aligned} \tag{4.1}$$

where we have set $\alpha = \mu_1 - 1$ and $\tau = \mu_2 + 1$. Linearizing (4.1) yields

$$\frac{\mathrm{d}}{\mathrm{d}t}x(t) = x(t) - x(t-1), \qquad \frac{\mathrm{d}}{\mathrm{d}t}\mu_1(t) = 0, \qquad \frac{\mathrm{d}}{\mathrm{d}t}\mu_2(t) = 0. \tag{4.2}$$

A basis for the centre subspace of the linear system (4.2) is

$$\Phi = \begin{pmatrix} 1 & \theta & 0 & 0 \\ 0 & 0 & 1 & 0 \\ 0 & 0 & 0 & 1 \end{pmatrix},$$

the bilinear form (3.6) reduces to

$$\langle \psi, \phi \rangle = \psi(0)\phi(0) - \int_{-1}^{0} \psi(\xi+1) \begin{pmatrix} 1 & 0 & 0 \\ 0 & 0 & 0 \\ 0 & 0 & 0 \end{pmatrix} \phi(\xi)\,\mathrm{d}\xi, \tag{4.3}$$

and it can easily be checked that the matrix

$$B = \begin{pmatrix} 0 & 1 & 0 & 0 \\ 0 & 0 & 0 & 0 \\ 0 & 0 & 0 & 0 \\ 0 & 0 & 0 & 0 \end{pmatrix}$$

satisfies relation (3.8). We write $z = [z_1, z_2, \mu_1, \mu_2]^{\mathrm{T}}$ for the coordinates on the centre manifold. Finally, we

note that the nonlinear terms in (4.1) are given by

$$F([v_1, v_2, v_3]^{\mathrm{T}}) = [v_3(0)(v_1(0) - v_1(-1)) + (1 + v_3(0))(v_2(0)v_1(-1) + \gamma_1 v_1(0)^3 + \gamma_2 v_1(0)^2 v_1(-1) + \gamma_3 v_1(0)v_1(-1)^2 + \gamma_4 v_1(-1)^3 + \mathrm{O}(|v|^5)), 0, 0]^{\mathrm{T}}. \tag{4.4}$$

Retaining up to first-order terms in $\mu_1$ and $\mu_2$, and up to third-order terms overall, we get the following truncated equations on the centre manifold

$$\frac{\mathrm{d}}{\mathrm{d}t} z_1 = z_2 + \tfrac{2}{3}[\mu_2 z_2 + \mu_1(z_1 - z_2) + a_1 z_1^3 + a_2 z_1^2 z_2 + a_3 z_1 z_2^2 + a_4 z_2^3], \tag{4.5}$$

$$\frac{\mathrm{d}}{\mathrm{d}t} z_2 = 2[\mu_2 z_2 + \mu_1(z_1 - z_2) + a_1 z_1^3 + a_2 z_1^2 z_2 + a_3 z_1 z_2^2 + a_4 z_2^3], \qquad \frac{\mathrm{d}}{\mathrm{d}t}\mu_1 = 0, \qquad \frac{\mathrm{d}}{\mathrm{d}t}\mu_2 = 0, \tag{4.6}$$

where

$$a_1 = \gamma_1 + \gamma_2 + \gamma_3 + \gamma_4, \tag{4.7}$$

$$a_2 = -\gamma_2 - 2\gamma_3 - 3\gamma_4, \tag{4.8}$$

$$a_3 = \gamma_3 + 3\gamma_4, \tag{4.9}$$

$$a_4 = -\gamma_4. \tag{4.10}$$

Eqs. (4.5) and (4.6) can be simplified by a near-identity transformation to normal form, given to third-order by

$$\frac{\mathrm{d}}{\mathrm{d}t} z_1 = z_2, \qquad \frac{\mathrm{d}}{\mathrm{d}t} z_2 = 2\left[\mu_2 z_2 + \mu_1\left(z_1 - \frac{2}{3} z_2\right) + (a_1 + a_2) z_1^2 z_2 + a_1 z_1^3\right]. \tag{4.11}$$

In terms of the original parameters, Eqs. (4.11) become

$$\frac{\mathrm{d}}{\mathrm{d}t} z_1 = z_2,$$

$$\frac{\mathrm{d}}{\mathrm{d}t} z_2 = (2\alpha + 2) z_1 + \left(-\frac{4\alpha}{3} + 2\tau - \frac{10}{3}\right) z_2 + 2(\gamma_1 - \gamma_3 - 2\gamma_4) z_1^2 z_2 + 2(\gamma_1 + \gamma_2 + \gamma_3 + \gamma_4) z_1^3. \tag{4.12}$$

It is well-known [25] that the normal forms for the Takens–Bogdanov singularity with reflectional symmetry are determined to cubic order and are given by

$$\frac{\mathrm{d}}{\mathrm{d}t} z_1 = z_2, \qquad \frac{\mathrm{d}}{\mathrm{d}t} z_2 = a z_1^3 + b z_1^2 z_2, \tag{4.13}$$

when $a$ and $b$ are both non-zero. The following two-parameter family then provides a versal unfolding for (4.13) [16, Section 7.3]

$$\frac{\mathrm{d}}{\mathrm{d}t} z_1 = z_2, \qquad \frac{\mathrm{d}}{\mathrm{d}t} z_2 = \beta_1 z_1 + \beta_2 z_2 + a z_1^3 + b z_1^2 z_2. \tag{4.14}$$

Thus, comparing (4.12) and (4.14), we can immediately read off the relations between the original DDE parameters $\alpha$, $\tau$, $\gamma_i$, $i = 1, \ldots, 4$ and the parameters $\beta_1$, $\beta_2$, $a$ and $b$ in the versal unfolding (4.14) of the Takens–Bogdanov singularity with reflectional symmetry.

Note that up to reflections and a reversal of time, there are precisely two topological normal forms in (4.14). These can be chosen to be the cases with (1) $a > 0$, $b < 0$, and (2) $a < 0$, $b < 0$. However, in our case time reversals are not possible since we are dealing with a DDE. Thus, we must also consider the two cases where $b > 0$.

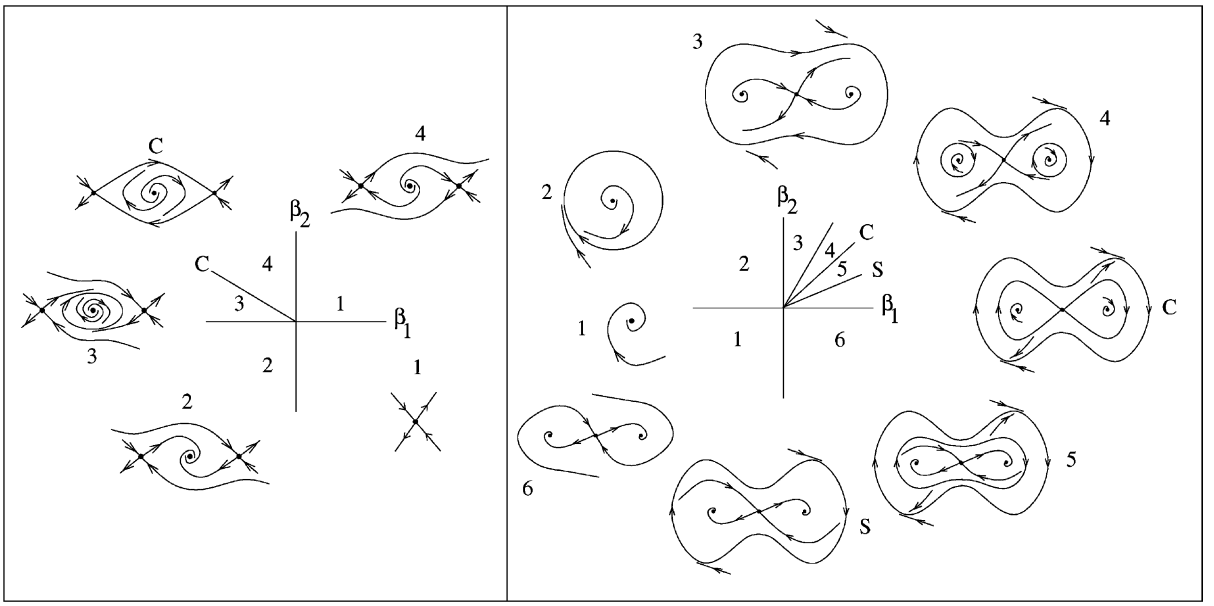


Fig. 2. Unfolding of both topological cases of the Takens–Bogdanov bifurcation with reflectional symmetry. All possible dynamics near the Takens–Bogdanov point (the origin in this figure) are summarized. In (a) we have $a > 0$, $b < 0$ and in (b) we have $a < 0$, $b < 0$ in Eq. (4.14).

However, it is easy to see that these are obtained from the two standard cases by merely reversing the direction of the flow, reflecting the phase space across the vertical axis, and reflecting the parameter space across the $\beta_1$-axis. We now consider each topological case individually.

*Case 1*: $a > 0$. In this case all possible dynamics near the Takens–Bogdanov point are summarized in Fig. 2a for the case $b < 0$ (reverse the direction of the arrows, reflect the phase space across the vertical axis and reflect the parameter space across the $\beta_1$-axis for the case $b > 0$). To first-order, the equation of the diagonal line in the second quadrant is [16, Section 7.3]

$$\beta_2 = -\frac{\beta_1}{5}. \tag{4.15}$$

The line $\beta_1 = 0$ is a pitchfork bifurcation line and the line $\beta_2 = 0$ ($\beta_1 < 0$) is a Hopf bifurcation line for the trivial equilibrium point.

*Case 2*: $a < 0$. In this case all possible dynamics near the Takens–Bogdanov point are summarized in Fig. 2 b for the case $b < 0$ (reverse the direction of the arrows, reflect the phase space across the vertical axis and reflect the parameter space across the $\beta_1$ axis for the case $b > 0$). To first-order, the equations of the diagonal lines (from top to bottom) are [16, Section 7.3]

$$\begin{aligned}
&\beta_2 = \beta_1 \quad \text{(Hopf bifurcation from non-trivial equilibria)},\\
&\beta_2 = \frac{4\beta_1}{5} \quad \text{(Line C : homoclinic connection of the trivial equilibrium)},\\
&\beta_2 = c\beta_1 \quad \text{(Line S : saddle-node of periodic orbits)}.
\end{aligned} \tag{4.16}$$

where $c \approx 0.752$. Furthermore, the line $\beta_1 = 0$ is a pitchfork bifurcation line and the line $\beta_2 = 0$ ($\beta_1 < 0$) is a Hopf bifurcation line for the trivial equilibrium point.

Thus, we have shown that if the cubic coefficients $\gamma_i$, $1 \leq i \leq 4$, in (1.2) satisfy the generic conditions

$$\gamma_1 + \gamma_2 + \gamma_3 + \gamma_4 \neq 0 \quad \text{and} \quad \gamma_1 - \gamma_3 - 2\gamma_4 \neq 0,$$

then the Takens–Bogdanov bifurcation in (1.2) is non-degenerate, and the dynamics of (1.2) near the trivial equilibrium and near the point $(\alpha, \tau) = (-1, 1)$ is reduced to one of the phase diagrams of Fig. 2, with a possible reversal of the arrows, regardless of the fifth- and higher order terms.

## 5. Applications

This section is devoted to the study of specific examples of Eq. (1.2) along with comparisons with numerical simulations. The simulations were done using a fixed-step fourth-order Runge–Kutta method with linear interpolation for the required two midpoint evaluations of the delayed variable. A range of time steps were used to ensure the accuracy of our simulations. In all cases, constant initial functions were used.

### 5.1. Example 1

The first case we study is that of a simple standard bistable system with delayed linear feedback. As mentioned in Section 1, such equations have received attention in the context of the ENSO phenomenon, where they serve as a simple heuristic model known as the delayed action oscillator [24]. It is also being investigated in the context of neural networks with intrinsic bistable elements. It has the form

$$\frac{\mathrm{d}}{\mathrm{d}t}x(t) = x(t) + \alpha x(t-\tau) - x(t)^3, \tag{5.1}$$

where $\alpha, \tau \in \mathbb{R}$, with $\tau > 0$. Note that this model is a special case of Eq. (1.2) with $(\gamma_1, \gamma_2, \gamma_3, \gamma_4) = (-1, 0, 0, 0)$. In the context of ENSO, the dependent variable $x$ represents the sea surface temperature (SST) anomaly. The first term on the right-hand side represents unstable ocean–atmosphere perturbations, while the third term represents the nonlinear effects that limit its growth (e.g. advective processes in the ocean and moist processes in the atmosphere). A side effect of the unstable ocean–atmosphere perturbations is the generation of oceanic waves. The delayed feedback term represents the effect of these oceanic waves (i.e., westward propagating Rossby waves on the ocean thermocline that, after reflecting from the western boundary, become eastward propagating Kelvin waves that re-enter the coupled ocean–atmosphere system after a time delay equal to their transit time).

Using the results of Section 4, we find that near the point $(\alpha, \tau) = (-1, 1)$ in parameter space equation (5.1) is well approximated near the trivial equilibrium by the centre manifold equations

$$\frac{\mathrm{d}}{\mathrm{d}t}z_1 = z_2, \qquad \frac{\mathrm{d}}{\mathrm{d}t}z_2 = (2\alpha + 2)z_1 + \left(-\frac{4\alpha}{3} + 2\tau - \frac{10}{3}\right)z_2 - 2z_1^2 z_2 - 2z_1^3. \tag{5.2}$$

In fact, based on numerical simulations, it appears that its global behaviour is well approximated by these equations also. We see that the coefficients in Eqs. (5.2) are such that they fall into Case 2 of the Takens–Bogdanov classification (see Fig. 2 b). Fig. 2 b predicts that in Region 4 we should see multistability. Using Eqs. (4.16) we see that the line $\beta_2 = 9\beta_1/10$ lies in Region 4. In terms of the original parameters this line becomes $\tau = 47\alpha/30 + 77/30$. The point $(\alpha, \tau) = (-19/20, 647/600)$ lies on this line (and in Region 4) and is close to the Takens–Bogdanov point. We therefore expect to see multistability in the DDE for these parameter values. Indeed, we see this multistability in Fig. 3; both the limit cycle and the non-trivial equilibria are stable.

As another example, consider the point $(\alpha, \tau) = (-10/9, 9/10)$. This point lies in Region 1 of Fig. 2 b. Here we expect to see only a stable trivial equilibrium in the DDE and, in fact, we see this in Fig. 4. Our approach using a

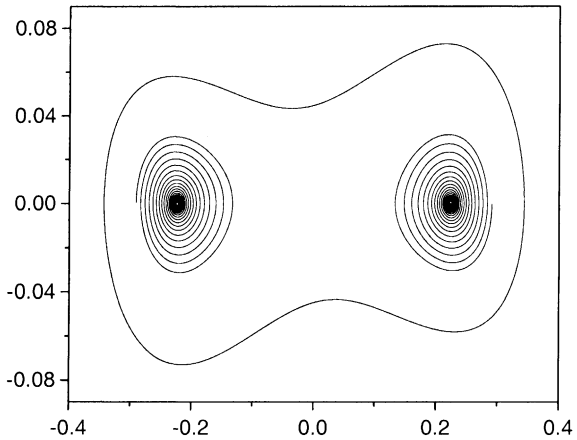


Fig. 3. Multistability: numerical simulation of (5.1) with $(\alpha, \tau) = (-19/20, 647/600)$. These parameter values fall in Region 4 of Fig. 2 b, where the DDE exhibits multistability. The vertical axis is $\dot{x}$ and the horizontal axis is $x$.

suspended system which includes the parameters as dynamic variables has enabled us to locate precisely where in parameter space the features described in Fig. 2 b occur. It also enables us to relate the physical parameters in the model to the unfolding parameters in Eq. (4.14).

### 5.2. Example 2

In Battisti and Hirst [1], the authors analyse a simple coupled ocean–atmosphere model. They argue that the essential physics in this model can be described by a linear delayed oscillator (the Suarez and Schopf model without the cubic nonlinearity). The authors identify the important nonlinearity in the full coupled model and derive the leading order nonlinear analog model for ENSO, which takes the form of a nonlinear DDE

$$\frac{\mathrm{d}}{\mathrm{d}t}x(t) = x(t) + \alpha x(t-\tau) - e[x - rx(t-\tau)]^3, \tag{5.3}$$

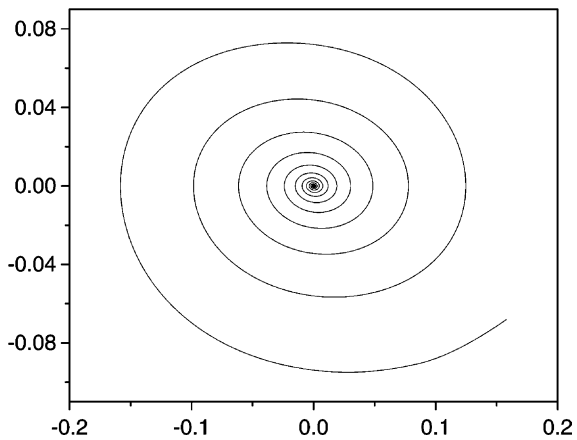


Fig. 4. Numerical simulation of (5.1) with $(\alpha, \tau) = (-10/9, 9/10)$. These parameter values fall in Region 1 of Fig. 2 b. In this region the DDE has only a stable trivial equilibrium. The vertical axis is $\dot{x}$ and the horizontal axis is $x$.

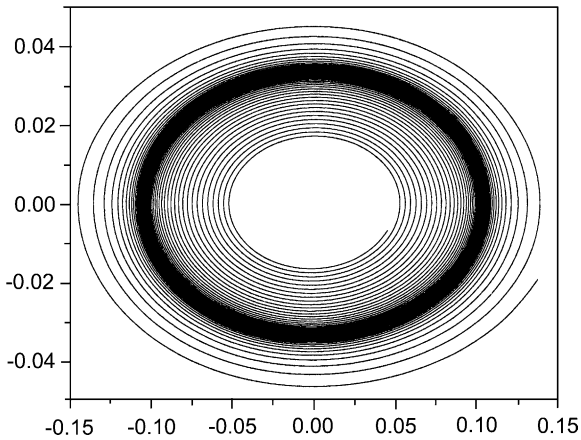


Fig. 5. Stable limit cycle: numerical simulation of (5.3) with $(\alpha, \tau) = (-20/19, 553/570)$. These parameter values fall in Region 3 of Fig. 2 a, where the DDE has a stable limit cycle. The vertical axis is $\dot{x}$ and the horizontal axis is $x$.

where $x$ represents the SST anomaly, $e$ and $r$ are positive real parameters, and $\alpha$ and $\tau$ are defined as above. Again, this model is a special case of Eq. (1.2) with $(\gamma_1, \gamma_2, \gamma_3, \gamma_4) = (-e, 3er, -3er^2, er^3)$. Although similar in form to the Suarez and Schopf model, the Battisti and Hirst model represents a different balance in the fundamental processes.

Once again, the results of Section 4 show that near the point $(\alpha, \tau) = (-1, 1)$ in parameter space Eq. (5.3) is well approximated near the trivial equilibrium by the centre manifold equations

$$\begin{aligned} &\frac{\mathrm{d}}{\mathrm{d}t} z_1 = z_2, \\ &\frac{\mathrm{d}}{\mathrm{d}t} z_2 = (2\alpha+2) z_1 + \left( -\frac{4\alpha}{3} + 2\tau - \frac{10}{3} \right) z_2 + (-e + 3er^2 - 2er^3) z_1^2 z_2 + (-e + 3er - 3er^2 + er^3) z_1^3. \end{aligned} \tag{5.4}$$

It can easily be shown that regardless of the value of the parameter $e$ in Eq. (5.3), the coefficient of the $z_1^2 z_2$ term in Eqs. (5.4) will be negative for all values of $r$, and that the coefficient of the $z_1^3$ term in Eqs. (5.4) will be negative if $r < 1$ and will be positive if $r > 1$. To summarize, if $r > 1$ then the dynamics near the TB point are described in Fig. 2 a, and if $r < 1$ then the dynamics near the TB point are described in Fig. 2 b. In [1], the authors use a value of $r$ that is less than 1. Their model therefore falls into Case 2 of the Takens–Bogdanov classification, but it is interesting to note that it can fall into Case 1 if we allow for a value of $r > 1$ (perhaps by choosing a different ocean "box" geometry). To illustrate this case we let $(e, r) = (1, 3/2)$, then the long term dynamics of this DDE near the Takens–Bogdanov point are summarized in Fig. 2 a. In Region 3 of Fig. 2 a we see that there is a stable limit cycle encircling the trivial equilibrium point. This limit cycle was found in the DDE for parameter values in Region 3 (see Fig. 5).

## 6. Conclusion

We have performed a bifurcation analysis of a class of first-order nonlinear DDEs with reflectional symmetry. Our results reveal the presence of a Takens–Bogdanov bifurcation point which acts as an organizing centre around the origin. Our results are also original in that they also provide the unfolding of this bifurcation in terms of the

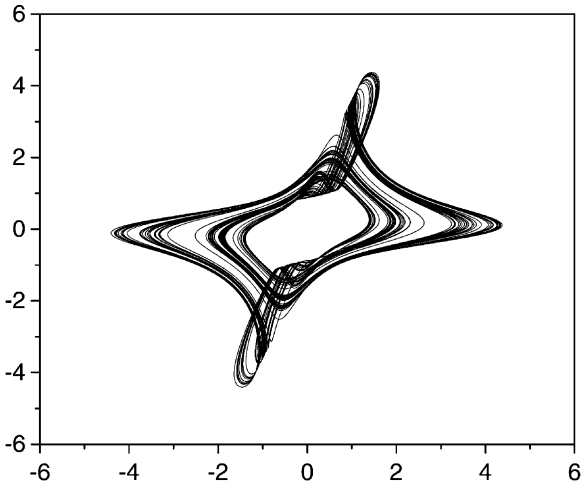


Fig. 6. Chaotic solution to the DDE? Numerical simulation of (6.1) with $(\alpha, \tau) = (-1.65, 0.705)$. The vertical axis is $x_\tau$ and the horizontal axis is $x$.

parameters of the original DDE. This was made possible due to our centre manifold analysis of the suspended DDE, i.e. of the DDE augmented with the (trivial) parameter dynamics.

Future work will address versions of Eq. (1.2) with multiple delays. It will also look into the origin of chaotic behaviour that we have found numerically. Specifically, consider the following DDE which is again a special case of Eq. (1.2) with $(\gamma_1, \gamma_2, \gamma_3, \gamma_4) = (0, -2, 1, 0)$

$$\frac{\mathrm{d}}{\mathrm{d}t}x(t) = x(t) + \alpha x(t-\tau) - 2x(t)^2 x(t-\tau) + x(t)x(t-\tau)^2. \tag{6.1}$$

Since $\gamma_1 - \gamma_3 - 2\gamma_4 = -1$ and $\gamma_1 + \gamma_2 + \gamma_3 + \gamma_4 = -1$, we fall into Case 2 of the Takens–Bogdanov classification (see Fig. 2 b). It can easily be verified with Eq. (3.29) that near the Takens–Bogdanov point the Hopf bifurcation is supercritical (i.e., the coefficient $a$ in Eq. (3.28) is negative). Far from this point, however, the criticality may change. In fact, the Hopf coefficient $a$ is positive if $\alpha < -1.65$ approximately. Near the point where the Hopf coefficient $a$ is null the DDE exhibits what seems to be chaotic behaviour. For example, let $(\alpha, \tau) = (-1.65, 0.705)$. Fig. 6 is a numerical simulation of the DDE with these parameter values.

This "chaotic" example shows that our analysis does not provide us with the full dynamical picture of this important class of DDEs and serves to remind us that there remains much to be studied. However, the analysis of this global behaviour is well beyond the scope of this paper.

## Acknowledgements

This work is funded in part by the Natural Sciences and Engineering Research Council of Canada.

## References

[1] D.S. Battisti, A.C. Hirst, Interannual variability in a tropical atmosphere–ocean model: influence of the basic state, ocean geometry and nonlinearity, J. Atmos. Sci. 46 (1989) 1687–1712.
[2] J. Bélair, Stability in a model of a delayed neural network, J. Dynam. Diff. Eq. 5 (1993) 6076–6123.

[3] J. Bélair, S.A. Campbell, Stability and bifurcations of equilibria in a multiple delayed differential equation, SIAM J. Appl. Math. 54 (1994) 1402–1424.
[4] N.J. Berman, L. Maler, Neural architecture of the electrosensory lateral line lobe: adaptations for coincidence detection, a sensory searchlight and frequency-dependent adaptive filtering, J. Exp. Biol. 202 (1999) 1243–1253.
[5] P.C. Bressloff, C.V. Wood, Spontaneous oscillations in a nonlinear delayed-feedback shunting model of the pupil light reflex, Phys. Rev. E 58 (1998) 3597–3606.
[6] P.C. Bressloff, S. Coombes, Symmetry and phase-locking in a ring of pulse-coupled oscillators with distributed delays, Physica D 126 (1999) 99–122.
[7] A.R. Bulsara, E. Jacobs, T. Zhou, F. Moss, L. Kiss, Stochastic resonance in a single neuron model: theory and analog simulation, J. Theor. Biol. 154 (1991) 531–555.
[8] S.A. Campbell, Stability and bifurcation of a simple neural network with multiple time delays, Fields Inst. Commun. 21 (1999) 65–79.
[9] J. Cao, Periodic oscillation and exponential stability of delayed cellular neural networks (CNN's), Phys. Lett. A 270 (2000) 157–163.
[10] V. Chinarov, M. Menzinger, Computational dynamics of gradient bistable networks, BioSystems 55 (2000) 137–142.
[11] S.-N. Chow, J.K. Hale, Methods of Bifurcation Theory, Springer, New York, 1982.
[12] T. Faria, L.T. Magalhães, Normal forms for retarded functional differential equations with parameters and applications to Hopf bifurcation, J. Diff. Eq. 122 (1995) 181–200.
[13] J.A. Freund, A.B. Neiman, L. Schimansky-Geier, Analytic description of noise-induced phase synchronization, Europhys. Lett. 50 (2000) 8–14.
[14] F. Giannakopoulos, A. Zapp, Local and global Hopf bifurcation in a scalar delay differential equation, J. Math. Anal. Appl. 237 (2) (1999) 425–450.
[15] K. Gopalsamy, I. Leung, Delay induced periodicity in a neural netlet of excitation and inhibition, Physica D 89 (1996) 395–426.
[16] J. Guckenheimer, P. Holmes, Nonlinear Oscillations, Dynamical Systems, and Bifurcations of Vector Fields, Springer, New York, 1983.
[17] J.K. Hale, Flows on centre manifolds for scalar functional differential equations, Proc. Roy. Soc. Edinb. A 101 (1985) 193–201.
[18] J.K. Hale, S.V. Lunel, Introduction to Functional Differential Equations, Springer, New York, 1993.
[19] M. Kim, et al., Controlling chemical turbulence by global delayed feedback: pattern formation in catalytic CO oxidation on Pt(1 1 0), Science 292 (2001) 1357–1360.
[20] J.F. Lindner, B.K. Meadows, W.L. Ditto, Array enhanced stochastic resonance and spatiotemporal synchronization, Phys. Rev. Lett. 75 (1995) 3–6.
[21] A. Longtin, A. Bulsara, D. Pierson, F. Moss, Bistability and the dynamics of periodically forced sensory neurons, Biol. Cybern. 70 (1994) 569–578.
[22] C.M. Marcus, R.M. Westerwelt, Stability of analog neural networks with delay, Phys. Rev. A 39 (1989) 347–359.
[23] T. Ohira, Y. Sato, Resonance with noise and delay, Phys. Rev. Lett. 82 (1999) 2811–2815.
[24] M.J. Suarez, P.L. Schopf, A delayed action oscillator for ENSO, J. Atmos. Sci. 45 (1988) 3283–3287.
[25] F. Takens, Forced oscillations and bifurcations, Commun. Math. Inst., Rijkuniversiteit Utrecht 3 (1974) 1–59.
[26] P. van den Driessche, J. Wu, X. Zou, Stabilization role of inhibitory self-connections in a delayed neural network, Physica D 150 (2001) 84–90.
[27] J. Wei, S. Ruan, Stability and bifurcation in a neural network model with two delays, Physica D 130 (1999) 255–272.
[28] J. Wu, Symmetric functional differential equations and neural networks with memory, Trans. Am. Math. Soc. 350 (1999) 4799–4838.